Widely Tunable Single-Photon Source from a Carbon Nanotube in the Purcell Regime

A. Jeantet,[1] Y. Chassagneux,[1] C. Raynaud,[1] Ph. Roussignol,[1] J. S. Lauret,[2] B. Besga,[3] J. Estève,[3] J. Reichel,[3] and C. Voisin[1,*]

[1]*Laboratoire Pierre Aigrain, École Normale Supérieure, CNRS, Université Pierre et Marie Curie,*
Université Paris Diderot, 24, rue Lhomond, F-75005 Paris, France
[2]*Laboratoire Aimé Cotton, CNRS, École Normale Supérieure de Cachan,*
Universite Paris Sud, 91405 Orsay, France
[3]*Laboratoire Kastler Brossel, École Normale Supérieure, CNRS, Université Pierre et Marie Curie,*
24 rue Lhomond, F-75005 Paris, France

The narrow emission of a single carbon nanotube at low temperature is coupled to the optical mode of a fiber microcavity using the built-in spatial and spectral matching brought by this flexible geometry. A thorough cw and time-resolved investigation of the very same emitter both in free space and in cavity shows an efficient funneling of the emission into the cavity mode together with a strong emission enhancement corresponding to a Purcell factor of up to 5. At the same time, the emitted photons retain a strong sub-Poissonian statistics. By exploiting the cavity feeding effect on the phonon wings, we locked the emission of the nanotube at the cavity resonance frequency, which allowed us to tune the frequency over a 4 THz band while keeping an almost perfect antibunching. By choosing the nanotube diameter appropriately, this study paves the way to the development of carbon-based tunable single-photon sources in the telecom bands.

Recent breakthroughs in the photophysics of carbon nanotubes have led to the observation of narrow-band excitonic emission and photon antibunching up to room temperature [1–5].

Therefore, coupling a single carbon nanotube to a photonic resonator is highly sought for technological developments [6–9] including for single-photon sources in view of quantum cryptography or quantum computation. In addition, the low cost, the high integrability, and the possible electrical excitation of nanotubes [10] are attractive assets in these perspectives. Such devices are also interesting for academic studies due to the original effects expected from the hybrid 1D–0D electronic behavior of carbon nanotubes [11]. However, due to the lack of control of the growth or deposition processes, current attempts rely on random spectral and spatial matching between a resonator (microdisks [12] or photonic crystals [13]) and randomly deposited nanotubes, putting strong limitations on the investigation of this technology.

In this work, we propose an original approach where the nanotube is fully characterized in free space by regular microphotoluminescence (micro-PL) spectroscopy and where a microcavity is subsequently formed around the emitter by approaching a concave dielectric mirror micro-engineered at the apex of an optical fiber. This geometry brings an invaluable flexibility giving a built-in spectral and spatial matching, together with excellent quality factors and mode volumes [14]. Individual carbon nanotubes were coupled to the cavity, resulting in a brightening of more than an order of magnitude. By means of time-resolved measurements, we were able to investigate directly the cavity-enhanced emission rate and found a Purcell factor F_p of up to 5 and an extraction efficiency of 80%. At the same time, we performed intensity correlation measurements and observed a strong sub-Poissonian statistic with $g^{(2)}(0) \leq 0.03$ both for the free space and cavity-enhanced emissions. Finally, by adjusting the cavity length, we were able to tune the working wavelength of the emitter over 15 meV (4 THz) while keeping the spectral width of the source below 300 μeV (80 GHz) by exploiting the cavity feeding effect [15] on the acoustic phonon sidebands [16]. This work shows the relevance of exploiting cavity quantum electrodynamical (CQED) effects to enhance the photonic properties of carbon nanotubes.

CoMoCat Single Wall carbon nanotubes (SWNTs) wrapped in PFO were dispersed in toluene with polystyrene and spun on a flat dielectric mirror resulting in a 120 nm thick layer. The nanotube concentration was lower than 0.1 μm^{-2}. Figure 1 shows a sketch of the experimental setup. All the measurements were conducted at 20 K. The sample was illuminated from the back with a cw or pulsed Ti:sapphire laser tuned beyond the edge of the stop band of the mirror at about 800 nm (nonresonant excitation of the nanotube) [17]. An aspherical lens was used to collect the near-infrared luminescence of individual nanotubes. The luminescence was further dispersed in a 500 mm spectrometer and detected with a nitrogen-cooled CCD camera. Once a nanotube was localized and characterized, the microcavity was formed by approaching the top mirror (50 μm radius of curvature), which is engineered at the apex of an optical fiber by means of CO_2 laser ablation [14]. In order to facilitate the positioning of the top mirror
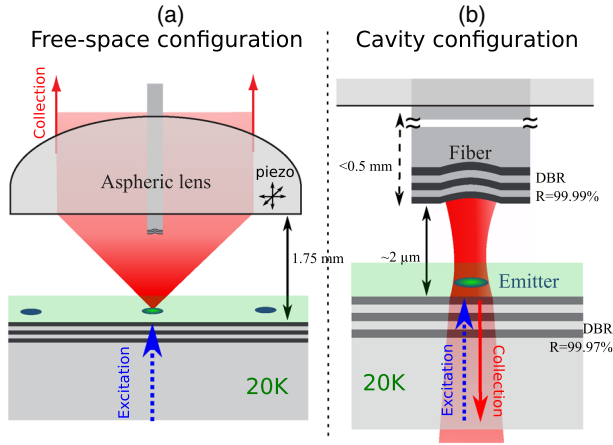
FIG. 1.   (a), (b) Sketch of the experimental setup showing the versatile micro-PL or scanning cavity microscope. DBR stands for Distributed Bragg Reflector.

with respect to the tube location, the fiber was inserted in the center of the aspherical lens used for the micro-PL measurements through a 400 μm hole. Importantly, the excitation through the back mirror is unchanged in the cavity configuration, which ensures that the very same nanotube is investigated. Finally, by choosing the reflectivities of the mirrors appropriately, we obtained an asymmetric Fabry-Perot with a preferential output (88%) through the back mirror. In the cavity configuration, the output photons are thus collected from the back through a second aspherical lens and a dichroic mirror. The finesse F of the cavity was set to about 6000 in order to match the quality factor of the emitter for an optimal coupling.

A typical micro-PL spectrum of an individual nanotube is shown in Fig. 2(c). The spectrum consists of a sharp (FWHM 500 μeV) zero-phonon line (ZPL) superimposed to acoustic phonon sidebands [16]. When closing the cavity, we observe a strong emission through the back mirror as long as the cavity length, and therefore the cavity resonant frequency is tuned in resonance with the ZPL [Fig. 2(a)]. In this configuration, the luminescence collected from the cavity consists of a sharp single line [FWHM 330 μeV ($\simeq$80 GHz)] showing a strong enhancement of the peak intensity as compared to the free-space configuration [Fig. 2(b)]. Note that for emitters broader than the cavity the proper way to show that the cavity acts beyond simple spectral filtering is to compare the photon spectral density [18]. We find a spectral density enhancement of the order of 20 for the tube of Fig. 2.

Let us first emphasize that the signal is collected through a highly reflective mirror, which is a direct proof of the coupling of the nanotube to the cavity mode. The 20-fold intensity enhancement results both from an intrinsic brightening of the emitter (Purcell effect) and from a better collection of the light emitted in the cavity mode. In fact, the emission diagram of the nanotube coupled to the cavity was measured from the far field image of the mode (see

Supplemental Material [19]). It shows an angular aperture lower than 9 deg, in good agreement with the one expected for the TEM00 cavity mode. This narrow emission angle allows an almost perfect collection, in contrast to the free-space configuration that shows a classical dipolar radiation pattern (modulated by interferences due to the back supporting mirror) leading to a collection efficiency of about 20% (see Supplemental Material [19]).

Taking into account these collection efficiencies and the transmission factors of all the optical parts [19], we obtain a first estimate of the intrinsic brightening of the nanotube, i.e., the enhancement of its radiative rate [24]. In fact, carbon nanotubes have a low radiative yield and any increase of the radiative rate directly translates into an equivalent increase of the brightness, even for an excitation well below the saturation. As a consequence, exploiting the Purcell effect to enhance the brightness of a single-photon source is especially relevant for such dim emitters. We can finally compare the spectrally integrated photon counts in both configurations, and we find a Purcell factor of the order of 3. The main uncertainty arises from the collection efficiency and leads to a global uncertainty on F_p of the order of 30% (see Supplemental Material [19]).

We now take advantage of the unique flexibility of this geometry to tune the length of the cavity over a wide range so as to change significantly the mode volume. The corresponding count rate is shown in Fig. 2(d) for multiple back and forth scans. The length of the cavity is increased by steps of $\lambda/2$ in order to stay in resonance with the ZPL of the emitter. The linear $1/V$ dependence of the count rate is directly related to the variation of the Purcell factor with the mode volume [see Eq. (2)].

Nevertheless, the most direct insight into the Purcell effect—as defined by the ratio of the radiative rate into the cavity mode to the free-space radiative rate—is obtained in the time domain, by means of time-resolved photoluminescence [25]. In the case of a low-yield emitter, however, the global lifetime is marginally modified due to the overwhelming nonradiative decay. More precisely, the Purcell factor F_p can be inferred from the relative change of lifetime through [26]

$$\tau_{\mathrm{cav}} = \frac{\tau_{\mathrm{fs}}}{1 + \eta F_p}, \qquad (1)$$

where τ_{cav} is the lifetime of the nanotube in the cavity, τ_{fs} is its lifetime in free space, and η is its free-space quantum radiative efficiency (i.e., radiative recombination rate over global recombination rate) [27]. Figure 3 shows time-resolved photoluminescence transients of a nanotube with and without the cavity. In order to account for the photon storage in the cavity, we separately recorded the decay of the cavity subsequent to a resonant pulsed excitation (see Supplemental Material [19]). We convoluted this photon storage decay with the free-space decay of the nanotube in order to properly compare the transients in the two

(a)
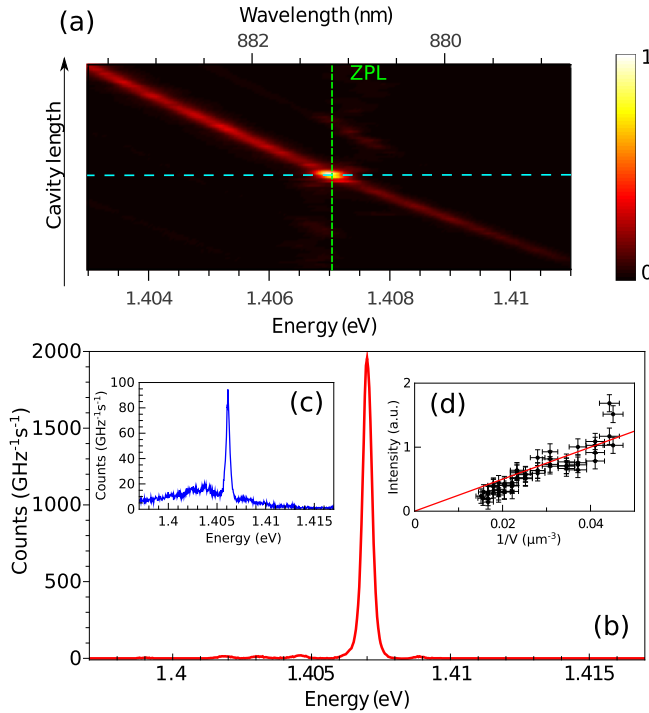
FIG. 2. (a) 2D plot of the emission spectrum of a nanotube embedded in the fiber microcavity. The color scale encodes the emission intensity while the horizontal axis corresponds to the wavelength and the vertical one to the cavity length. The green dashed line corresponds to the ZPL wavelength, while the light blue one corresponds to the resonant cavity length. (b) Emission spectrum (photon · $GHz^{-1} s^{-1}$) of the nanotube when the cavity is tuned in resonance with its ZPL [horizontal cut of (a) along the blue dashed line]. (c) Free-space luminescence spectrum of the same nanotube. (d) Integrated count rate as a function of the mode volume when the cavity length is increased by steps of $\lambda/2$.

configurations. Figure 3 unambiguously shows a reduction of lifetime of the emitter when coupled to the cavity, which is a direct signature of the Purcell effect. The numerical fits of these transients yield $\tau_{\mathrm{cav}} = 183 \pm 4$ ps, $\tau_{\mathrm{fs}} = 203 \pm 4$ ps. Thus, we deduce that the relative change of lifetime induced by the cavity is $10 \pm 3\%$.

The radiative quantum yield of this emitter was estimated through saturation measurements in pulsed excitation (inset of Fig. 3). In fact, in the saturation regime, one and only one excitation is created in the emitting state for each pulse (see intensity correlation measurements below). Therefore, the count rate divided by the repetition rate of the excitation yields the radiative efficiency of the effective two-level system. For the particular nanotube of Fig. 3, we find $\eta \simeq 2 \pm 0.5\%$, which is consistent with the literature [29].

In total, these time-resolved measurements bring a direct demonstration of a sizable Purcell effect with carbon nanotubes, with a Purcell factor F_p of 5 ± 2 for the nanotube of Fig. 3 [30]. This value corresponds to a sixfold enhancement of the radiative yield of the nanotube, bringing its value close to 12%. Furthermore, the corresponding coupling factor $\beta = F_p/(1 + F_p)$ shows that 80% of the
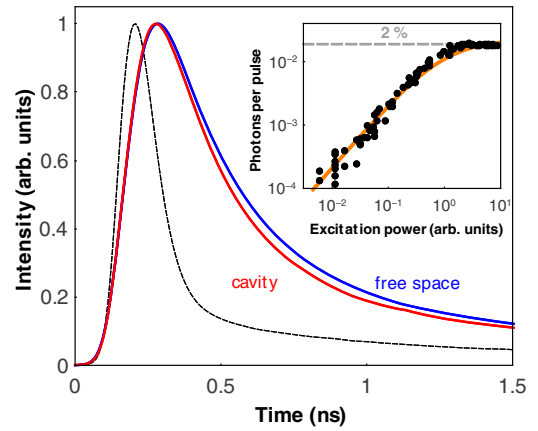
FIG. 3. Time-resolved photoluminescence of a nanotube in free space (blue line) or coupled to a resonant cavity (red line). Response of the detector (dashed line). The free-space transient was convoluted with the empty cavity response (not shown) in order to account for the photon storage time in the cavity. Inset: Saturation measurement of the same nanotube measured in free space under pulsed excitation.

photons emitted by the nanotube are effectively extracted through the cavity mode.

This F_p value is in line with the theoretical value (assuming a nanotube placed at a field maximum) given by [32]

$$F_p = \frac{3}{4\pi^2} \frac{(\lambda/n)^3}{V} Q_{\mathrm{eff}}, \qquad (2)$$

where V is the mode volume, n is the optical index at the position of the emitter, and Q_{eff} is the effective quality factor of the system $[(1/Q_{\mathrm{eff}}) = (1/Q_{\mathrm{cav}}) + (1/Q_{\mathrm{em}})]$. The cavity length (and thus the mode volume) can be extracted from the free spectral range (see Supplemental Material [19]), the effective quality factor is deduced from white-light transmission measurements for the cavity contribution Q_{cav}, while the dephasing rate γ^* of the emitter (and thus $Q_{\mathrm{em}} = (\omega_{\mathrm{ex}}/\gamma^*)$) is measured from the FWHM of the ZPL ($\hbar\gamma^* = 300$ μeV for the nanotube of Fig. 3). We obtain $F_p^{\mathrm{th}} = 5$, in good agreement with the experimental value. Interestingly, the strength of the coupling of the emitter to the confined optical mode can also be expressed in terms of the cavity-emitter coupling factor (or vacuum Rabi splitting) g, which can be compared to the other energy scales of the system. Using $F_p = 4g^2/(\gamma_R \gamma^*)$, where γ_R stands for the radiative rate, and Eq. (1), we deduce $g = (1/2)\sqrt{\gamma^*(\tau_{\mathrm{fs}} - \tau_{\mathrm{cav}})/(\tau_{\mathrm{cav}}\tau_{\mathrm{fs}})}$. We obtain $\hbar g \sim 7 \pm 2$ μeV for the nanotube of Fig. 3 [33].

We performed such measurements on about a dozen nanotubes (see Supplemental Material [19]). We consistently find a relative reduction of lifetime of the order of 5%–15%, while the free-space radiative yield spans the [0.5–5]% range, leading to Purcell factors between 1 and 15. This dispersion was expected since the radiative yield is
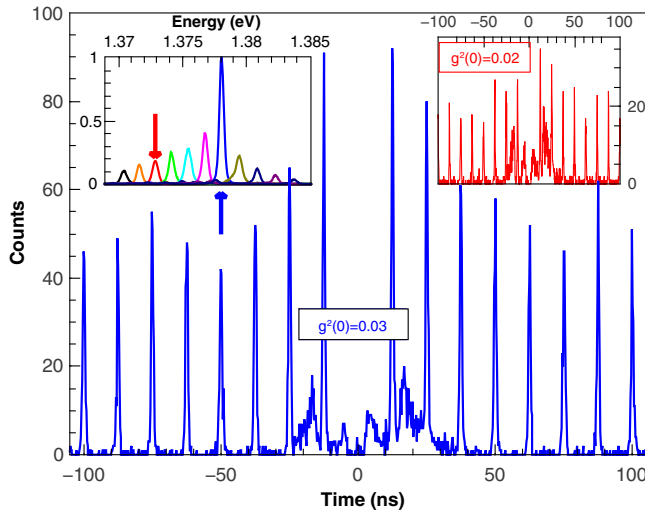
FIG. 4.   Intensity correlation measurements of a nanotube resonantly coupled to a fiber cavity obtained in a Hanbury Brown–Twiss setup under pulsed excitation. The missing peak at time 0 $[g^{(2)}(0) = 0.03]$ shows that high-quality single photons are emitted by the nanotube. The signal between the first and second peaks corresponds to detector artifacts (afterpulses). Right inset: Same measurements for a detuning of the cavity corresponding to an emission of the phonon side wings. Left inset: Output of the cavity for several detunings. The corresponding intensity correlations are displayed in the main panel and in the right inset according to the color code of the arrows.

known to be highly sensitive to defects and environment. Similarly, we found a coupling g ranging from 7 to 30 μeV. Note that the best values of g lie only within a factor of 5 below the linewidth γ^* of the narrowest nanotubes observed in this study, putting the strong coupling in reach for reasonable improvements of the system.

We now investigate the quantum properties of the source made of the nanotube resonantly coupled to the cavity by measuring the intensity correlations in a Hanbury Brown–Twiss setup (Fig. 4) [34]. Free-space emission of carbon nanotubes at low temperature is known to show strong antibunching [1]. However, the microscopic mechanism responsible for such photon statistics in a one-dimensional emitter is still a debated issue [1,5]. Despite the strong spectral filtering of the emission in the cavity, we observe that this peculiar photon statistics is preserved with an almost full suppression of multiple photon emission probability $[g^{(2)}(0) \sim 0.03]$. This paves the way to the use of cavity embedded nanotubes as near-infrared single-photon sources. In particular, nanotubes with slightly larger diameter (1.1 nm versus 0.7 nm for the SWNTs used in this study to match spectral detectivity of our photon counting module) could be used for sources in the telecom bands where alternative emitters are scarce. In fact, it was shown that such nanotubes emitting in the telecom C band are ruled by the same photophysics [11].

Interestingly, the emission enhancement is not limited to the ZPL and we can make use of the phonon sidebands to efficiently feed the cavity in a spectral window as broad as 15 meV (4 THz). This effect is shown in the left-hand inset of Fig. 4, where the spectrum of the light collected from the cavity is displayed for several detunings, within the same longitudinal mode. This shows the ability of carbon nanotubes to be used as widely tunable single-photon sources. In fact, as can be seen in the right-hand inset of Fig. 4, the source retains its ability to emit single photons all throughout the 15 meV range of tunability. The origin of this efficient cavity feeding is not completely clear yet, but it could be related to the nature of the phonon wings. In fact, these wings imply long-lived acoustic phonons that do not introduce additional dephasing (in contrast to optical phonon replica [18]). Therefore, the coupling of the wings to the optical mode is expected to be comparable to the one of the ZPL [35].

In conclusion, we have demonstrated that single-wall carbon nanotubes can be efficiently coupled to a microcavity to reach up to a 20-fold brightness enhancement. Using an original approach where the microcavity can be formed on a specific emitter after a full free-space characterization, we were able to perform a thorough investigation of the Purcell increase of the radiative rate due to the optical confinement. Finally, we have shown that the acoustic phonon sidebands in the luminescence spectra of carbon nanotubes can be exploited to feed the cavity over a broad spectral range, providing an original means to implement a widely tunable single-photon source. This study paves the way to many developments in exploiting CQED effects with carbon nanotubes by improving both the nanotube and the cavity. For instance, the use of slightly larger diameter nanotubes could provide efficient single-photon sources operating at telecom wavelengths, whereas a reduction of the mode volume should put the strong coupling regime in reach, opening the way to hybrid excitations with a marked one-dimensional component.

─────────

*Corresponding author.
christophe.voisin@lpa.ens.fr
[1] A. Högele, C. Galland, M. Winger, and A. Imamoglu, Phys. Rev. Lett. **100**, 217401 (2008).
[2] W. Walden-Newman, I. Sarpkaya, and S. Strauf, Nano Lett. **12**, 1934 (2012).
[3] T. Endo, J. Ishi-Hayase, and H. Maki, Appl. Phys. Lett. **106**, 113106 (2015).
[4] X. Ma, N. F. Hartmann, J. K. S. Baldwin, S. K. Doorn, and H. Htoon, Nat. Nanotechnol. **10**, 671 (2015).

[5] X. Ma, O. Roslyak, J. G. Duque, X. Pang, S. K. Doorn, A. Piryatinski, D. H. Dunlap, and H. Htoon, Phys. Rev. Lett. **115,** 017401 (2015).

[6] F. Xia, M. Steiner, Y.-m. Lin, and P. Avouris, Nat. Nanotechnol. **3,** 609 (2008).

[7] R. Watahiki, T. Shimada, P. Zhao, S. Chiashi, S. Iwamoto, Y. Arakawa, S. Maruyama, and Y. K. Kato, Appl. Phys. Lett. **101,** 141124 (2012).

[8] D. Legrand, C. Roquelet, G. Lanty, P. Roussignol, X. Lafosse, S. Bouchoule, E. Deleporte, C. Voisin, and J. S. Lauret, Appl. Phys. Lett. **102,** 153102 (2013).

[9] A. Noury, X. L. Roux, L. Vivien, and N. Izard, Nanotechnology **25,** 215201 (2014).

[10] L. Marty, E. Adam, L. Albert, R. Doyon, D. Ménard, and R. Martel, Phys. Rev. Lett. **96,** 136803 (2006).

[11] V. Ardizzone, Y. Chassagneux, F. Vialla, G. Delport, C. Delcamp, N. Belabas, E. Deleporte, P. Roussignol, I. Robert-Philip, C. Voisin, and J. S. Lauret, Phys. Rev. B **91,** 121410 (2015).

[12] S. Imamura, R. Watahiki, R. Miura, T. Shimada, and Y. K. Kato, Appl. Phys. Lett. **102,** 161102 (2013).

[13] R. Miura, S. Imamura, R. Ohta, A. Ishii, X. Liu, T. Shimada, S. Iwamoto, Y. Arakawa, and Y. K. Kato, Nat. Commun. **5** (2014).

[14] D. Hunger, T. Steinmetz, Y. Colombe, C. Deutsch, T. W. Hänsch, and J. Reichel, New J. Phys. **12,** 065038 (2010).

[15] A. Auffèves, J.-M. Gérard, and J.-P. Poizat, Phys. Rev. A **79,** 053838 (2009).

[16] F. Vialla, Y. Chassagneux, R. Ferreira, C. Roquelet, C. Diederichs, G. Cassabois, P. Roussignol, J.-S. Lauret, and C. Voisin, Phys. Rev. Lett. **113,** 057402 (2014).

[17] F. Vialla, E. Malic, B. Langlois, Y. Chassagneux, C. Diederichs, E. Deleporte, P. Roussignol, J.-S. Lauret, and C. Voisin, Phys. Rev. B **90,** 155401 (2014).

[18] R. Albrecht, A. Bommer, C. Deutsch, J. Reichel, and C. Becher, Phys. Rev. Lett. **110,** 243602 (2013).

[19] See Supplemental Material at http://link.aps.org/supplemental/10.1103/PhysRevLett.116.247402, which includes Refs. [20–23], for further analysis of the PL

transients; statistical aspects; emission diagram and collection efficiency; mode volume computation.

[20] A. Auffèves, D. Gerace, J.-M. Gérard, M. F. Santos, L. C. Andreani, and J.-P. Poizat, Phys. Rev. B **81,** 245419 (2010).

[21] Y. Murakami and J. Kono, Phys. Rev. Lett. **102,** 037401 (2009).

[22] A. Yariv, *Quantum Electronics* (Wiley, New York, 1989).

[23] A. F. Oskooi, D. Roundy, M. Ibanescu, P. Bermel, J. D. Joannopoulos, and S. G. Johnson, Comput. Phys. Commun. **181,** 687 (2010).

[24] Broadband excitation was used in this measurement to eliminate residual interference effects in the excitation density [see also the absence of modulation in Fig. 2(d)].

[25] J. M. Gérard, B. Sermage, B. Gayral, B. Legrand, E. Costard, and V. Thierry-Mieg, Phys. Rev. Lett. **81,** 1110 (1998).

[26] A. Faraon, P. E. Barclay, C. Santori, K.-M. C. Fu, and R. G. Beausoleil, Nat. Photonics **5,** 301 (2011).

[27] This result is obtained in the approximation where the emission in the leaky modes remains comparable to the free-space emission rate. This holds in our geometry where the cavity mode is viewed by the emitter through a small solid angle [28].

[28] D. J. Heinzen, J. J. Childs, J. E. Thomas, and M. S. Feld, Phys. Rev. Lett. **58,** 1320 (1987).

[29] S. Berger, C. Voisin, G. Cassabois, C. Delalande, P. Roussignol, and X. Marie, Nano Lett. **7,** 398 (2007).

[30] Similar Purcell enhancement factors were recently reported with a plasmonic approach, but at the expense of spectral purity and emission directionality [31].

[31] N. Mauser, N. Hartmann, M. S. Hofmann, J. Janik, A. Högele, and A. Hartschuh, Nano Lett. **14,** 3773 (2014).

[32] E. M. Purcell, Phys. Rev. **69,** 674 (1946).

[33] Note that this value of g is independent of any calibration of the setup (and in particular of the radiative quantum yield).

[34] P. Michler, A. Kiraz, C. Becher, W. V. Schoenfeld, P. M. Petroff, L. Zhang, E. Hu, and A. Imamoglu, Science **290,** 2282 (2000).

[35] U. Hohenester, A. Laucht, M. Kaniber, N. Hauke, A. Neumann, A. Mohtashami, M. Seliger, M. Bichler, and J. J. Finley, Phys. Rev. B **80,** 201311 (2009).